Molecular Basis of the Time-Dependent Inhibition of Cyclooxygenases by Indomethacin†

Jeffery J. Prusakiewicz, Andrew S. Felts, Bonnie S. Mackenzie, and Lawrence J. Marnett*

A. B. Hancock, Jr., Memorial Laboratory for Cancer Research, Departments of Biochemistry and Chemistry, Vanderbilt Institute for Chemical Biology, Center in Molecular Toxicology, and Vanderbilt-Ingram Comprehensive Cancer Center, Vanderbilt University School of Medicine, Nashville, Tennessee 37232

Received July 11, 2004; Revised Manuscript Received September 5, 2004

ABSTRACT: Cyclooxygenases (COXs) are the therapeutic targets of nonsteroidal antiinflammatory drugs. Indomethacin (INDO) was one of the first nonsteroidal antiinflammatory drugs to be characterized as a time-dependent, functionally irreversible inhibitor, but the molecular basis of this phenomenon is uncertain. In the crystal structure of INDO bound to COX-2, a small hydrophobic pocket was identified that surrounds the 2′-methyl group of INDO. The pocket is formed by the residues Ala-527, Val-349, Ser-530, and Leu-531. The contribution of this pocket to inhibition was evaluated by altering its volume by mutagenesis of Val-349. The V349A mutation expanded the pocket and increased the potency of INDO, whereas the V349L mutation reduced the size of the pocket and decreased the potency of INDO. Particularly striking was the reversibility of INDO inhibition of the V349L mutant. The 2′-*des*-methyl analogue of INDO (DM-INDO) was synthesized and tested against wild-type COX-1 and COX-2, as well as the Val-349 mutants. DM-INDO bound to all enzymes tested, but only inhibited wt mCOX-2 and the V349I enzyme. Without the 2′-methyl group anchoring DM-INDO in the active site, the compound was readily competed off of the enzyme by arachidonic acid. The kinetics of inhibition were comparable to the kinetics of binding as evaluated by fluorescence quenching. These results highlight binding of the 2′-methyl of INDO in the hydrophobic pocket as an important determinant of its time-dependent inhibition of COX enzymes.

Cyclooxygenases (COX-1 and COX-2)[1] are the molecular targets for several of the beneficial pharmacological actions of nonsteroidal antiinflammatory drugs (NSAIDs), as well as their principal undesirable side effects (*1*−*3*). Detailed investigations of the kinetics of inhibition reveal that many NSAIDs interact with COX-1 and COX-2 via a multistep mechanism in which an initial rapid, reversible step is followed by one or more slow and poorly reversible steps (eq 1) (*4*, *5*). The magnitude of the rate constants for the

$$E + I \underset{k_{-1}}{\overset{k_1}{\rightleftharpoons}} E{-}I \underset{k_{-2}}{\overset{k_2}{\rightleftharpoons}} E{-}I^* \qquad K_I = k_{-1}/k_1 \qquad (1)$$

reverse reaction is a major determinant of the tightness of binding and therefore the potency of inhibition. Aspirin and indomethacin (INDO) were the first two compounds found to display this multistep mechanism, but many other compounds exhibit similar kinetics of inhibition including the COX-2-selective NSAIDs, celecoxib and rofecoxib (*6*, *7*). The latter compounds employ a third, time-dependent step that is responsible for their COX-2 selectivity (*8*, *9*).

The molecular basis for the time dependence of some COX inhibitors has been established. Aspirin covalently modifies COX-1 and COX-2 by acetylating Ser-530, thereby irreversibly inhibiting the enzymes (*10*−*12*). During the third step of binding, celecoxib and rofecoxib insert sulfonamide and sulfone groups, respectively, into a side pocket near the base of the active site, which is only accessible in COX-2 (*13*). Diclofenac coordinates its carboxyl group to adjacent hydroxyls provided by Tyr-385 and Ser-530 (*14*). Interestingly, the molecular basis for time-dependent inhibition by INDO is not completely understood, despite the fact that it was first described more than 30 years ago. Rome and Lands demonstrated that converting the carboxyl group of indomethacin into a methyl ester renders it a reversible, competitive inhibitor of COX-1, but the same and similar transformations do not abolish time-dependent inhibition of COX-2 (*5*, *15*, *16*).

Kurumbail et al reported the crystal structure of INDO bound to COX-2 (*13*). Given the time required for crystallization, it is likely that this represents the structure of the tightly bound complex. Inspection of the structure reveals that the 2′-methyl group on the indole ring of INDO inserts into a hydrophobic pocket lining the COX-2 active site. This pocket is comprised of the side chains of Val-349, Ala-527, Ser-530, and Leu-531, which are conserved between isoforms (Figure 1A,B). We hypothesized that interactions with this small hydrophobic pocket are an important determinant of the tight-binding of INDO to COX enzymes and that the time dependence reflects, in part, the establishment of these

† This research was supported in part by National Institutes of Health Research Grant CA89450, Center Grants CA68484 and ES0026N, and Training Grant GM65086 (A.S.F.).

* Corresponding author. Telephone: (615)-343-7329. Fax: (615)-343-7534. E-mail: larry.marnett@vanderbilt.edu.

[1] Abbreviations: COX, cyclooxygenase; AA, arachidonic acid; NSAID, nonsteroidal antiinflammatory drug; INDO, indomethacin; DM-INDO, 2′-*des*-methyl-indomethacin: mCOX, murine COX; oCOX, ovine COX; DMSO, dimethyl sulfoxide; wt, wild-type.

10.1021/bi048534q CCC: $27.50
Published on Web 11/17/2004

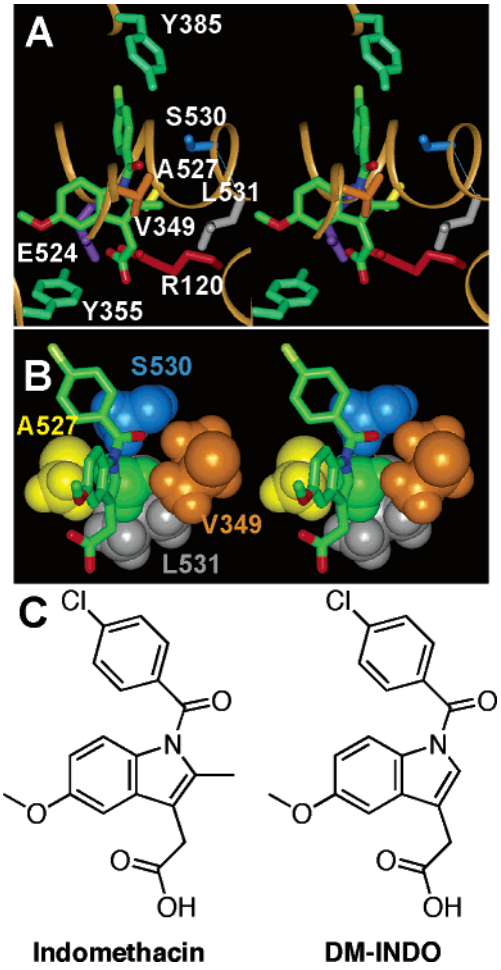

FIGURE 1: Crystal structure of INDO bound in the COX-2 active site. Stereoviews of INDO cocrystallized with COX-2 (Protein Data Bank code 4COX) (*13*) show (A) key active site residues for catalysis and the binding of ligands, (B) space-filling model of the 2′-methyl substituent of INDO (green) inserted into the hydrophobic pocket formed by Val-349, Ala-527, Ser-530, and Leu-531. Panel C shows the chemical structures of INDO and DM-INDO.

interactions. Therefore, we mutated Val-349 to residues with smaller or larger side chains and determined the kinetics of binding and inhibition of the mutant proteins. We also synthesized a 2-*des*-methyl-INDO analogue and evaluated its interaction with wild-type (wt) and mutant COXs. The results of our investigations strongly support a role for the hydrophobic pocket in the time-dependent inhibition of COX-1 and COX-2 by INDO.

EXPERIMENTAL PROCEDURES

Materials. Unlabeled arachidonic acid (AA) was purchased from Nu Chek Prep (Elysian, MN), and [1-^{14}C]-AA was purchased from PerkinElmer Life Sciences Inc. (Boston, MA). Ram seminal vesicles were purchased from Oxford Biomedical Research (Oxford, MI). Oligonucleotides were purchased from Operon Technologies (Alameda, CA), and all molecular biology enzymes were obtained from New England Biolabs (Beverly, MA). Baculovirus reagents were purchased from Pharmingen (San Diego, CA). Unless otherwise stated, all other chemicals were obtained from Sigma/Aldrich (St. Louis, MO). The synthetic scheme for preparation of DM-INDO and chemical characterization data are provided in Supporting Information.

Enzymology. Site-directed mutagenesis, expression, and purification of murine COX-2 were performed as previously described (*17*). All proteins were over 80% pure. Quantification of cyclooxygenase activity was performed in a thermostated cuvette at 37 °C and monitored using a polarographic electrode with a YS5300 oxygen monitor (Yellow Springs Instrument Co. Inc., Yellow Springs, OH). All inhibitors and substrates were solubilized in dimethyl sulfoxide (DMSO). Activity or inhibition assays were performed in 100 mM Tris-HCl buffer containing 500 μM phenol with hematin-reconstituted protein. Maximal reaction velocity data were obtained from the linear portion of the oxygen uptake curves, and the data were analyzed by nonlinear regression with Prism 4.0 (GraphPad Software, San Diego, CA). Competitive inhibition assays were performed in a similar manner, except substrate and inhibitor were added prior to the initiation of the reaction by addition of protein. The peroxidase activity of purified proteins was measured by the guaiacol method as described previously (*18*). The K_m's and V_{max}'s for COX activity and the relative peroxidase activity of COX-2 mutants are reported in Supporting Information (Table 5).

COX Inhibition Screening Assay. Reactions were run with reconstituted protein at final concentrations adjusted to give approximately 40% substrate consumption (oCOX-1 = 35 nM, wt mCOX-2 = 55 nM, V349A = 250 nM, V349I = 250 nM, and V349L = 100 nM). Time-dependent inhibition reactions were performed by preincubating the inhibitor and enzyme for 17 min at 25 °C, followed by 3 min at 37 °C prior to the addition of 50 μM [1-^{14}C]-AA for 30 s at 37 °C. Assays were terminated and analyzed for substrate consumption by thin-layer chromatography as previously described (*16*). All inhibitor concentrations for 50% enzyme activity (IC_{50}) were determined graphically and were the average of at least two independent determinations.

Time-Dependent COX Inhibition Assays. Enzymes at the concentrations listed above, were preincubated at 37 °C for varying lengths of time (0 s, 15 s, 30 s, 45 s, 1 min, 3, min, 5, min, 15 min, and 30 min) with various concentrations of INDO. All reactions were performed with [1-^{14}C]-AA for 30 s at 37 °C; reactions were terminated and analyzed as described above. For time-dependent inhibition assays of DM-INDO monitored by oxygen uptake, 50 nM mCOX-2 or 100 nM V349L were preincubated with inhibitor (0−200 μM) at 37 °C for various times (0, 1, 2, 5, 7, 10, 15, 30, and 60 s), followed by the addition of 50 μM AA. The values of kinetic parameters were the average of at least two independent determinations.

Reversibility of COX Inhibition by INDO and DM-INDO. Reactions were conducted under similar conditions as the time-dependent IC_{50} assay. Enzymes at the concentrations stated above were preincubated at 25 °C for 17 min with DMSO, 10 μM INDO, or 10 μM DM-INDO prior to 3 min at 37 °C. Cyclooxygenase reactions were initiated by the addition of 50 μM [1-^{14}C]-AA. Aliquots were removed at specific time points (30 s to 5 min) and added to tubes containing termination solution. Substrate consumption was analyzed by thin-layer chromatography and normalized to the appropriate DMSO control (*16*).

Steady-State Quenching of COX Intrinsic Fluorescence. Fluorescence quenching experiments with INDO and DM-INDO were performed with a Spex Fluorolog-3 spectrofluorometer as outlined previously (*19*). The ligands were

Table 1: Time-dependent IC_{50} Determinations (μM) of INDO and DM-INDO[a]

enzyme	INDO	DM-INDO
V349A	0.08	>16
wt mCOX-2	0.25	4
V349I	0.45	3
V349L	4	>16
wt oCOX-1	0.04	>16

[a] Values are the average of two independent determinations as outlined in Experimental Procedures.

dissolved in DMSO before further dilution into buffer. The organic component in the buffer was below 0.4%. The excitation (280 nm) and emission (327 nm) bandwidths were 4 and 6 nm, respectively. Steady-state measurements were performed at 37 °C in a 3.5 mL fluorescence cuvette with continuous stirring. All apo-proteins were diluted to 200 nM and displayed less than 2% activity of an equivalent amount of holoenzyme. Data were collected over 240 or 360 s with 2 s integration times. The reversibility of quenching was analyzed in the same manner with subsequent addition of 50 μM AA as competitor. Proteins were mixed with either INDO or DM-INDO for 240 s, and binding was monitored by intrinsic fluorescence quenching of COX. After each incubation, we attempted to chase the quencher off of the proteins by the addition of AA (50 μM) as a nonquenching competitor. Incubations were normalized to the DMSO control and fit to a single exponential. The dependence of k_{obs} on the INDO and DM-INDO concentrations was graphed in a secondary plot for the forward reaction (k_{on}) and the reverse reaction (k_{off}). The k_{on} data were analyzed by nonlinear regression with eq 2, and the k_{off} data were analyzed by linear regression to determine the binding constants.

RESULTS

Time-Dependent COX Inhibition by INDO. To investigate the interactions of the 2′-methyl group with the small hydrophobic pocket, a series of mutations were made at position 349 to increase or decrease the volume of the pocket (valine to alanine, isoleucine, or leucine), and the kinetics of inhibition of these enzymes by INDO were determined. Initially, a time-dependent IC_{50} assay was used, in which the enzymes were preincubated with inhibitor for 20 min before the addition of 50 μM AA. The COX reaction was allowed to proceed for 30 s before termination. The IC_{50} values indicated that the potency of INDO increased when the volume of the pocket increased (V349A) and decreased when the volume of the pocket decreased (V349I, V349L) (Table 1).

The time dependence of inhibition of wt and mutant COXs by INDO was determined by adding AA (50 μM) to the various enzyme preparations following preincubation with INDO for different times. To ensure that pseudo-first-order conditions were maintained, the enzymatic oxygenation reactions were terminated after 30 s to prevent extensive consumption of substrate. The decline of substrate conversion at different INDO concentrations was plotted against the preincubation times and fit to a single-exponential decay with a plateau to determine k_{obs} (Figure 2). The time-dependent inhibition curves for wt mCOX-2 approached 0% remaining activity. The graphs for V349A and V349I also approached 0% remaining activity, although V349A displayed a faster rate of inhibition (data not shown). V349L approached a nonzero asymptote of nearly 20% remaining activity, which suggested that the second step of binding was reversible (Figure 2C). The dependence of k_{obs} on the INDO concentration for the two-step, time-dependent mechanism (eq 1) is represented by eq 2 (*20*).

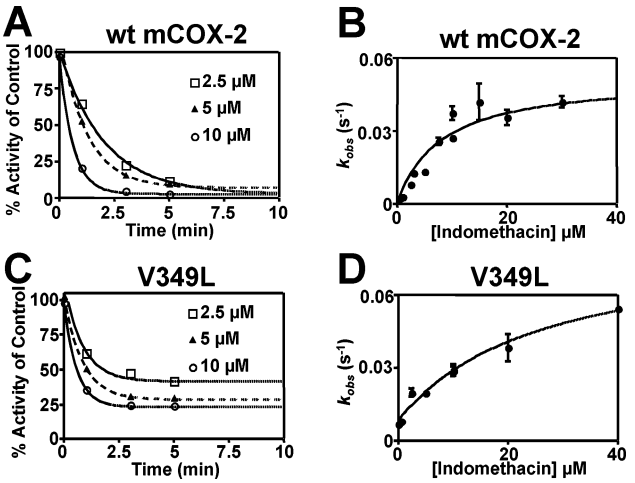

FIGURE 2: Kinetics of the time-dependent inhibition of COX-2 mutants by INDO. Assays were performed as described in Experimental Procedures. Representative data are expressed as percent activity of the uninhibited control with nonlinear regression curves. Proteins were preincubated with inhibitors for various times (0 s, 15 s, 30 s, 45 s, 1 min, 3, min, 5, min, 15 min, and 30 min) before the addition of substrate. For clarity, a limited number of data points are shown on each curve. The curves drawn as secondary plots for panels B and D were generated by fitting data to eq 2.

Table 2: Kinetic Parameters of Time-Dependent Inhibition by INDO[a]

enzyme	K_I, μM	k_2, s^{-1}	k_{-2}, s^{-1}	k_{-2},[b] s^{-1}
V349A	1.9 ± 0.4	0.074 ± 0.005	*c*	*c*
wt mCOX-2	7.9 ± 2.2	0.052 ± 0.005	*c*	*c*
V349I	5.3 ± 1.8	0.045 ± 0.004	*c*	*c*
V349L	26 ± 10	0.074 ± 0.013	0.008 ± 0.002	0.010 ± 0.002

[a] Kinetic parameters ±SE were determined from inhibition assays outlined in Experimental Procedures and shown in Figure 2. [b] Rate constant determined by reversible inhibition as outlined in Experimental Procedures and shown in Figure 3A. [c] Values were not detectable.

$$k_{obs} = \frac{k_2[I]}{(K_I + [I])} + k_{-2} \quad (2)$$

The rate constant k_2 represents the limiting forward rate constant for inhibition, and K_I corresponds to the inhibitor concentration that yields a rate equal to half of the limiting rate. The reverse rate constant of the second step, k_{-2}, is equal to the *y*-intercept and is equal to zero for compounds that display functionally irreversible inhibition. For wt mCOX-2, V349A, and V349I enzymes, the *y*-intercept was effectively zero (Figure 2B). In contrast, the secondary plot of data for V349L exhibited a nonzero *y*-intercept, which was equal to k_{-2}.

Kinetic parameters for wt mCOX-2 (Table 2) were in good agreement with previously reported values of K_I (5 μM) and k_2 (0.045 s^{-1}) (*21*). The values for oCOX-1 indicate that INDO displayed higher affinity ($K_I = 1.7$ μM) and a faster

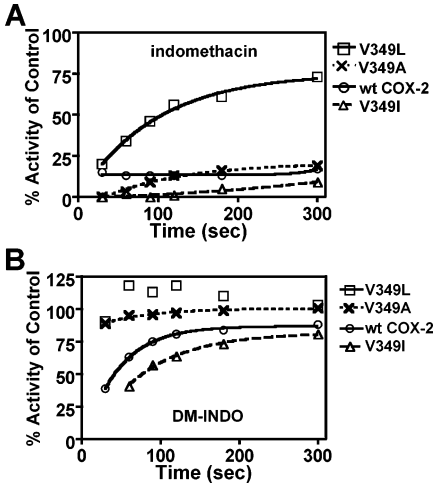

FIGURE 3: Effects of mutations on the reversibility of COX-2 inhibition by INDO and DM-INDO. Assays were performed with 10 μM of either INDO or DM-INDO as described in Experimental Procedures. Representative data are expressed as percent activity of the uninhibited control.

rate of inactivation ($k_2 = 0.25$ s^{-1}) (*22*). These observations are further supported by the higher potency of INDO toward oCOX-1 compared to mCOX-2 (Table 1). The K_I of V349A for INDO decreased almost 4-fold, which suggested a higher affinity of binding. This mutation also slightly increased k_2, which corresponded to the 3-fold reduction in the IC_{50} value for INDO against the V349A enzyme (Table 1). As noted in Table 1, the V349I mutation had little effect on the kinetic parameters of INDO. V349L demonstrated the greatest impact on inhibition, increasing K_I 3-fold and introducing a measurable k_{-2}.

Reversibility of COX Inhibition by INDO. To test the reversibility of INDO inhibition, we exposed wt mCOX-2 and the three Val-349 mutants to the same conditions used for the time-dependent IC_{50} assay. The enzymes were preincubated for 20 min with DMSO or 10 μM INDO prior to the addition of 50 μM AA. After addition of AA, the oxygenation reactions were allowed to proceed for varying lengths of time. As the reaction time increased, the extent of inhibition decreased if INDO binding was reversible. The time course for recovery of AA oxygenation was fit to a single exponential (Figure 3A). As anticipated, significant reversibility of INDO inhibition was observed for the V349L mutant but not for wt, V349A, or V349I enzymes. The value of k_{-2} calculated from the activity recovery assay (0.01 s^{-1}) corresponded closely to the k_{-2} value calculated from the time-dependent inhibition assay for INDO (0.008 s^{-1}) (Table 2). This relationship suggested that the reversibility of the second step in the time-dependent mechanism is the principle determinant of inhibition by INDO in the presence of 50 μM AA.

Time-Dependent COX Inhibition by DM-INDO. The experiments described above suggested that insertion of the 2′-methyl group of INDO into the hydrophobic pocket is an important contributor to the time dependence of inhibition. To further test this, we synthesized DM-INDO (Figure 1C). In the time-dependent IC_{50} assay, DM-INDO weakly inhibited wt mCOX-2 and V349I but exhibited less than 20% inhibition of V349A, V349L, and wt oCOX-1 (Table 1). The time and concentration dependence of inhibition of wt enzyme and the V349L mutant exhibited a plateau of about

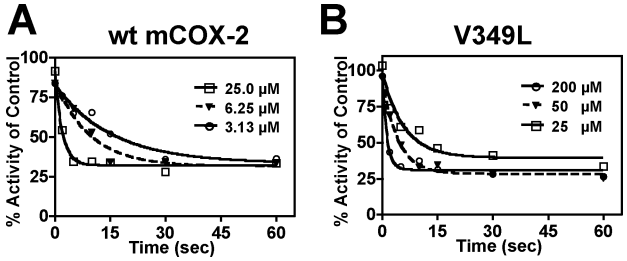

FIGURE 4: Kinetics of the time-dependent inhibition of COX-2 mutants by DM-INDO. Assays were performed as described in Experimental Procedures. Representative data are expressed as percent activity of the uninhibited control with nonlinear regression curves.

30% remaining activity for both enzymes, consistent with an appreciable k_{-2} (Figure 4). Importantly, V349L required nearly 10-fold higher concentrations of DM-INDO to achieve similar levels of inhibition to those observed with wt mCOX-2. Analysis of the data for inhibition of wt enzyme by DM-INDO yielded values for K_I, k_2, and k_{-2} of 26 $\pm$ 7 μM, 0.80 $\pm$ 0.03 s^{-1}, and 0.05 $\pm$ 0.02 s^{-1}, respectively. Thus, the on-rate constant (k_2) is 14-fold faster for DM-INDO than INDO and the off-rate constant (k_{-2}) is only 14-fold slower than the on-rate.

The kinetic data of V349L inhibition by DM-INDO were not amendable to analysis using eq 2, because the graph did not plateau (data not shown). Linear regression analysis yielded a *y*-intercept value for k_{-2} of 0.0025 $\pm$ 0.0003 s^{-1} (*23*). The K_I of DM-INDO for V349L must have been much greater than the equilibrium constant for the second step. Therefore, the first step in eq 1 was not saturated to allow for the time-dependent isomerization of E−I to E−I* (*23*).

Reversibility of COX Inhibition by DM-INDO. The reversibility of DM-INDO inhibition was evaluated similarly to INDO using the activity recovery assay (Figure 3). The experiments and analysis were performed as described above. DM-INDO displayed reversibility of inhibition for wt mCOX-2 and V349I with the k_{-2} values of 0.023 $\pm$ 0.001 and 0.015 $\pm$ 0.005 s^{-1}, respectively (Figure 3B). The small amount of activity lost for V349A and V349L by preincubation with 10 μM DM-INDO was quickly recovered upon addition of 50 μM AA (Figure 3B).

Quenching of COX Intrinsic Fluorescence by INDO and DM-INDO. Houtzager et al monitored inhibitor binding to COX-2 by fluorescence quenching of the apo-protein and demonstrated that the binding kinetics closely resembled the inhibition kinetics (*19*). This assay provided a method to directly monitor the binding of INDO and DM-INDO to COXs. Various concentrations of INDO and DM-INDO were added to apo-proteins, and the rate of fluorescence decrease was monitored over time (Figure 5A). After the mixture reached equilibrium, 50 μM of AA was added as competitor to monitor the reversibility of binding (Figure 5B). The kinetic data for quenching were analyzed in the same manner as those for inhibition. In a typical analysis, the traces were first averaged and then fit to a single exponential to calculate k_{obs}. Then, the dependence of k_{obs} on the quencher concentration was graphed in a secondary plot; an example analysis is shown for DM-INDO quenching of wt mCOX-2 in Figure 5C. Experimental parameters pertaining to the forward rate of quenching were termed k_{on}, and these data were fit with eq 2 to calculate kinetic binding constants. The reverse rates

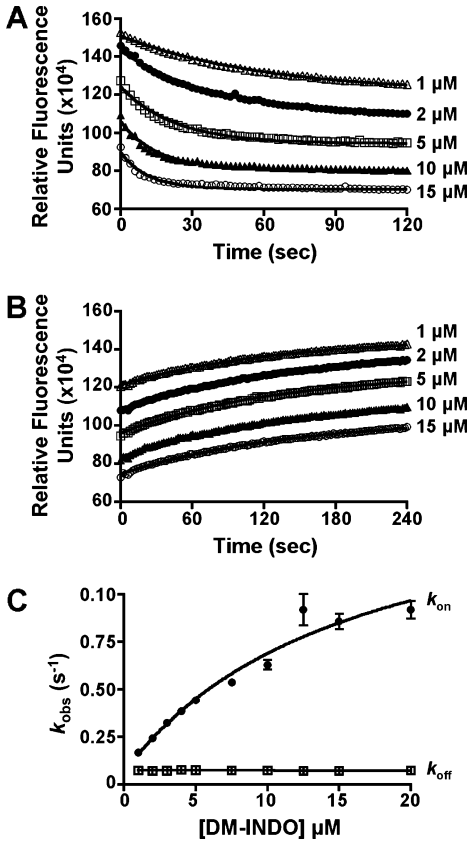

FIGURE 5: DM-INDO binding to apo-COX-2 monitored by fluorescence quenching. Assays were performed under conditions described in Experimental Procedures. In panel A, wt mCOX-2 (0.2 μM) was mixed with DM-INDO (1−20 μM) for 240 s. In panel B, DM-INDO was chased off of the protein by the addition of AA (50 μM) as a nonquenching competitor. The average of triplicate incubations were normalized to the DMSO control and fit to a single exponential (line). In panel C, The dependence of k_{obs} on the DM-INDO concentration was graphed in a secondary plot for the forward reaction (k_{on}) and the reverse reaction (k_{off}). The k_{on} data were analyzed by nonlinear regression with eq 2, and the k_{off} data were analyzed by linear regression to determine the binding constants.

Table 3: Kinetic Parameters of Fluorescence Quenching by INDO[a]

enzyme	K_d, μM	k'_2, s^{-1}	k'_{-2}, s^{-1}	k'_{-2},[b] s^{-1}
V349A	1.2 ± 0.3	0.12 ± 0.01	*c*	*c*
wt oCOX-1	3.9 ± 0.9	0.16 ± 0.02	*c*	*c*
wt mCOX-2	12 ± 3	0.062 ± 0.009	*c*	*c*
V349I	12 ± 2	0.078 ± 0.008	*c*	*c*
V349L	15 ± 6	0.065 ± 0.012	0.0016 ± 0.0002	0.0020 ± 0.0001

[a] Kinetic parameters ±SE were determined from fluorescence quenching assays outlined in Experimental Procedures. [b] Rate constant measured by fluorescence increase from competition with 50 μM AA outlined in Experimental Procedures. Averaged traces are shown in Figure 7. [c] Values were not detectable.

(k_{off}) of DM-INDO quenching of wt mCOX-2 showed no dependence on DM-INDO concentration (Figure 5B,C) and were analyzed by linear regression yielding a *y*-intercept equal to the reverse rate constant of the second step (k'_{-2}) (Table 3). For clarity, the equilibrium constant for the first step of fluorescence quenching is referred to as K_d, and k_2 and k_{-2} from the second step of quenching are represented by k'_2 and k'_{-2}, respectively.

As expected, INDO bound in a time-dependent fashion and was functionally irreversible for all enzymes except V349L; the latter displayed reversible, time-dependent binding (Figure 6). In agreement with the kinetics of inhibition, INDO quenched the V349A mutant and wt oCOX-1 more

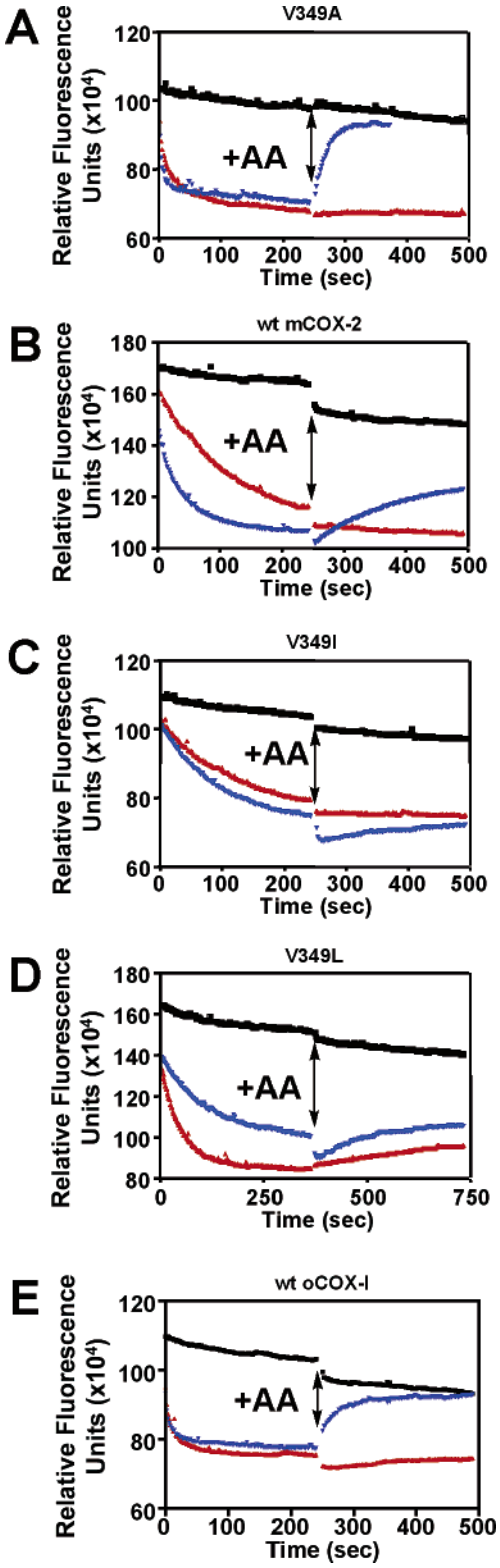

FIGURE 6: Fluorescence quenching of apo-COXs by INDO compared to DM-INDO and competition by AA. Assays were performed under conditions described in Experimental Procedures. Apo-protein at 0.2 μM was mixed with DMSO (black), INDO (red), or DM-INDO (blue) for 240 s (panels A−C and E) or 360 s (panel D), followed by the addition of 50 μM AA (arrow) and monitored for another 240 s (panels A−C and E) or 360 s (panel D). The final concentrations of INDO and DM-INDO were (A) 1, (B) 2, (C) 3, (D) 5, and (E) 1 μM. Traces are the average of three determinations.

Table 4: Kinetic Parameters of Fluorescence Quenching by DM-INDO[a]

enzyme	K_d, μM	k'_2, s^{-1}	k'_{-2}, s^{-1}	k'_{-2},[b] s^{-1}
V349A	1.4 ± 0.3	0.17 ± 0.04	0.045 ± 0.008	0.046 ± 0.002
wt oCOX-1	14 ± 3	0.28 ± 0.02	0.086 ± 0.026	0.033 ± 0.008
wt mCOX-2	16 ± 9	0.16 ± 0.04	0.006 ± 0.002	0.007 ± 0.001
V349I	12 ± 5	0.09 ± 0.01	0.003 ± 0.002	0.005 ± 0.001
V349L	34 ± 19	0.05 ± 0.01	0.003 ± 0.002	0.006 ± 0.001

[a] Kinetic parameters ±SE were determined from fluorescence quenching assays outlined in Experimental Procedures. [b] Rate constants measured by fluorescence increase from competition with 50 μM AA outlined in Experimental Procedures. Averaged traces are shown in Figure 7.

quickly than wt mCOX-2 (Figure 6). The kinetic parameters (K_d, k'_2) for INDO binding to V349A and wt oCOX-1 were very close between enzymes (Table 3). These effects on binding agree with the similar inhibitory potency observed in the time-dependent IC_{50} assay (Table 1). In fact, the kinetics of INDO binding to wt oCOX-1 agree very well with previously observed kinetics of inhibition ($K_I = 1.7$ μM, $k_2 = 0.25$ s^{-1}) (*22*). As suggested from inhibition studies, wt mCOX-2 bound INDO similarly to V349I. Further consistency between the binding and inhibition assays was established by the observation that AA could only compete INDO off V349L but not the other proteins (Figure 6D). The kinetic parameters derived from INDO quenching corresponded very well to those measured for INDO inhibition (Tables 2 and 3).

DM-INDO displayed reversible, time-dependent binding with all five enzymes in the quenching assay (Figure 6). The V349A mutation increased the rate of binding of DM-INDO and also increased the apparent affinity (K_d) (Table 4). Strikingly, the value k'_{-2} for V349A was 7-fold higher than that observed for wt mCOX-1 (Table 4). DM-INDO bound to wt oCOX-1 with kinetic constants appearing between those of V349A and wt mCOX-2. The k'_{-2} value for wt oCOX-1 was only slightly higher than that for V349A and wt mCOX-2 (Table 4). The K_d for wt oCOX-1 resembled that of wt mCOX-2, but the values of k'_{-2} for wt oCOX-1 were closer to the k'_{-2} value of V349A. The magnitude of these rate constants (k'_{-2}) helps to explain why little or no inhibition was observed despite the fact that DM-INDO binds to wt oCOX-1 and V349A. DM-INDO displayed a slightly smaller off-rate constant (k'_{-2}) for V349I than wt mCOX-2, which corresponded to the slight difference in the activity recovery assay observed between these two enzymes (Table 4, Figure 3B). As with INDO, DM-INDO bound reversibly to the V349L enzyme (Figure 5, 6). For each enzyme and inhibitor examined the values of k'_{-2} measured by fluorescence decay and calculated from eq 2 were equal to the k'_{-2} values measured by fluorescence recovery upon incubation with AA (Tables 3 and 4). Overall, the fluorescence quenching kinetics agreed well with the kinetics of inhibition.

DISCUSSION

INDO is a powerful COX inhibitor that is widely used for biochemical, cellular, and experimental animal investigations and is approved for human use in the treatment of rheumatoid and osteoarthritis and for reduction of pain associated with bursitis. INDO is a prototypical slow, tight-binding inhibitor that exhibits dramatically increased potency of COX inhibition after a several minute incubation with either COX isoform. The present experiments reveal that a principal determinant of the time-dependent increase in potency is the insertion of the 2′-methyl group into a hydrophobic pocket in the side of the COX active site. Alteration in the size of this pocket of COX-2 by site-directed mutagenesis of Val-349 alters the kinetics of inhibition and the kinetics of binding as evaluated by fluorescence quenching analysis. Particularly dramatic is the alteration in the kinetics of INDO interactions observed for the V349L mutant. This protein displayed significantly reduced sensitivity to inhibition by INDO and reversibility in both its binding and inhibition. The V349A mutant was actually more sensitive to inhibition by INDO than wild-type COX-2, which was due to a somewhat increased limiting rate for inhibition (k_2). Interestingly, the V349I mutant behaved more similarly to the V349A and wild-type enzymes than to the V349L enzyme. Inspection of the crystal structure in Figure 1 suggests that, if the terminal methyl group of isoleucine rotates away from the hydrophobic pocket, then the V349I mutant could still accommodate the 2′-methyl group of INDO (Figure 1B). This possibility must not be available for the V349L protein.

A hallmark of INDO inhibition of COX enzymes is that it appears to be functionally irreversible. Removal of the 2′-methyl group from INDO significantly reduces its potency as an inhibitor of COX-2 and COX-1 and eliminates its ability to serve as a functionally irreversible inhibitor. In fact, ovine COX-1 does not appear to be inhibited at all by DM-INDO at concentrations up to 16 μM. Although the 2′-methyl group appears to be a key contributor to time-dependent COX inhibition, it is not the sole determinant of binding. Previous studies have demonstrated that the carboxyl group of the indole-3-acetic acid moiety and the halogen atom of the *p*-chlorobenzoyl group also contribute to COX inhibition by INDO (*5*). Esterification or amidation of the carboxyl group transforms the molecule into a weak, reversible inhibitor of COX-1 but does not eliminate time-dependent inhibition of COX-2 (*5*, *16*). However, the mode of binding of INDO esters and amides appears to be different from that of the parent acid. Inhibition of COX-2 by INDO is eliminated by mutations of Arg-120 or Tyr-355, whereas inhibition by INDO esters and amides is eliminated by mutations of Tyr-355 or Glu-524 but not Arg-120 (16). The absence of a strong ionic interaction may account for the slow reversibility of inhibition observed for certain INDO amides containing bulky substituents in the amide functional group and for the inability of 2′-*des*-methyl derivatives of INDO esters and amides to exhibit any inhibition of COX-2 (*20*, *24*).

The present study reiterates the importance of Val-349 in the interaction of COX enzymes with substrates and inhibitors. Previous studies have revealed that mutations of Val-349 affect the affinities of COX-1 or COX-2 for substrates, the rates of substrate oxygenation, and the regiochemistry and stereochemistry of product formation (*25*, *26*). The decreases in specific activity observed with the various mutants in the present study are consistent with previous reports. The reduced activities of the mutants necessitated the adjustment of protein concentration in the inhibition assays to amounts that yielded similar rates of substrate turnover. However, a constant protein concentration was used in the fluorescence quenching assays because differences in

specific activities were irrelevant due to the use of apoenzyme. Despite the differences in protein concentrations and other aspects in the design of the inhibition and fluorescence quenching assays, the values determined for the kinetic parameters of INDO and DM-INDO binding and inhibition were remarkably consistent with the exception of the rate constants for dissociation where differences of less than 7-fold were observed.

Pharmacological activities of INDO such as its antiinflammatory activity, analgesic activity, and gastrointestinal toxicity are believed to derive from the ability of INDO to inhibit COX-2 and COX-1. However, INDO has been reported to exert additional biochemical activities in cellular systems, and it has been proposed that these non-COX activities may contribute to its in vivo pharmacology (*27*). Our observation that a subtle chemical modification, removal of the 2′-methyl group, greatly reduces COX inhibitory activity may provide a strategy for optimizing pharmacological effects at COX-independent targets while minimizing undesirable side effects due to COX inhibition.

ACKNOWLEDGMENT

We are grateful to K. L. Fillgrove for helpful discussions.

SUPPORTING INFORMATION AVAILABLE

The synthetic scheme for DM-INDO and the specific activities of the mutants. This material is available free of charge via the Internet at http://pubs.acs.org.

REFERENCES

1. Vane, J. R. (1971) Inhibition of prostaglandin synthesis as a mechanism of action for aspirin-like drugs, *Nat. New Biol. 231*, 232−235.
2. Smith, W. L., DeWitt, D. L., and Garavito, R. M. (2000) Cyclooxygenases: structural, cellular, and molecular biology, *Annu. Rev. Biochem. 69*, 145−182.
3. Kurumbail, R. G., Kiefer, J. R., and Marnett, L. J. (2001) Cyclooxygenase enzymes: catalysis and inhibition, *Curr. Opin. Struct. Biol. 11*, 752−760.
4. Smith, W. L., and Lands, W. E. (1971) Stimulation and blockade of prostaglandin biosynthesis, *J. Biol. Chem. 246*, 6700−6702.
5. Rome, L. H., and Lands, W. E. (1975) Structural requirements for time-dependent inhibition of prostaglandin biosynthesis by antiinflammatory drugs, *Proc. Natl. Acad. Sci. U.S.A. 72*, 4863−4865.
6. Copeland, R. A., Williams, J. M., Giannaras, J., Nurnberg, S., Covington, M., Pinto, D., Pick, S., and Trzaskos, J. M. (1994) Mechanism of selective inhibition of the inducible isoform of prostaglandin G/H synthase, *Proc. Natl. Acad. Sci. U.S.A. 91*, 11202−11206.
7. Ouellet, M., and Percival, M. D. (1995) Effect of inhibitor time-dependency on selectivity towards cyclooxygenase isoforms, *Biochem. J. 306* (Part 1), 247−251.
8. Lanzo, C. A., Beechem, J. M., Talley, J., and Marnett, L. J. (1998) Investigation of the binding of isoform-selective inhibitors to prostaglandin endoperoxide synthases using fluorescence spectroscopy, *Biochemistry 37*, 217−226.
9. Walker, M. C., Kurumbail, R. G., Kiefer, J. R., Moreland, K. T., Koboldt, C. M., Isakson, P. C., Seibert, K., and Gierse, J. K. (2001) A three-step kinetic mechanism for selective inhibition of cyclooxygenase-2 by diarylheterocyclic inhibitors, *Biochem. J. 357*, 709−718.
10. Roth, G. J., Stanford, N., and Majerus, P. W. (1975) Acetylation of prostaglandin synthase by aspirin, *Proc. Natl. Acad. Sci. U.S.A. 72*, 3073−3076.
11. Van Der Ouderaa, F. J., Buytenhek, M., Nugteren, D. H., and Van Dorp, D. A. (1980) Acetylation of prostaglandin endoperoxide synthetase with acetylsalicylic acid, *Eur. J. Biochem. 109*, 1−8.
12. DeWitt, D. L., el-Harith, E. A., Kraemer, S. A., Andrews, M. J., Yao, E. F., Armstrong, R. L., and Smith, W. L. (1990) The aspirin and heme-binding sites of ovine and murine prostaglandin endoperoxide synthases, *J. Biol. Chem. 265*, 5192−5198.
13. Kurumbail, R. G., Stevens, A. M., Gierse, J. K., McDonald, J. J., Stegeman, R. A., Pak, J. Y., Gildehaus, D., Miyashiro, J. M., Penning, T. D., Seibert, K., Isakson, P. C., and Stallings, W. C. (1996) Structural basis for selective inhibition of cyclooxygenase-2 by antiinflammatory agents, *Nature 384*, 644−648.
14. Rowlinson, S. W., Kiefer, J. R., Prusakiewicz, J. J., Pawlitz, J. L., Kozak, K. R., Kalgutkar, A. S., Stallings, W. C., Kurumbail, R. G., and Marnett, L. J. (2003) A novel mechanism of cyclooxygenase-2 inhibition involving interactions with Ser-530 and Tyr-385, *J. Biol. Chem. 278*, 45763−45769.
15. Greig, G. M., Francis, D. A., Falgueyret, J. P., Ouellet, M., Percival, M. D., Roy, P., Bayly, C., Mancini, J. A., and O'Neill, G. P. (1997) The interaction of arginine 106 of human prostaglandin G/H synthase-2 with inhibitors is not a universal component of inhibition mediated by nonsteroidal antiinflammatory drugs, *Mol. Pharmacol. 52*, 829−838.
16. Kalgutkar, A. S., Crews, B. C., Rowlinson, S. W., Marnett, A. B., Kozak, K. R., Remmel, R. P., and Marnett, L. J. (2000) Biochemically based design of cyclooxygenase-2 (COX-2) inhibitors: facile conversion of nonsteroidal antiinflammatory drugs to potent and highly selective COX-2 inhibitors, *Proc. Natl. Acad. Sci. U.S.A. 97*, 925−930.
17. Rowlinson, S. W., Crews, B. C., Lanzo, C. A., and Marnett, L. J. (1999) The binding of arachidonic acid in the cyclooxygenase active site of mouse prostaglandin endoperoxide synthase-2 (COX-2). A putative L-shaped binding conformation utilizing the top channel region, *J. Biol. Chem. 274*, 23305−23310.
18. Markey, C. M., Alward, A., Weller, P. E., and Marnett, L. J. (1987) Quantitative studies of hydroperoxide reduction by prostaglandin H synthase. Reducing substrate specificity and the relationship of peroxidase to cyclooxygenase activities, *J. Biol. Chem. 262*, 6266−6279.
19. Houtzager, V., Ouellet, M., Falgueyret, J. P., Passmore, L. A., Bayly, C., and Percival, M. D. (1996) Inhibitor-induced changes in the intrinsic fluorescence of human cyclooxygenase-2, *Biochemistry 35*, 10974−10984.
20. Timofeevski, S. L., Prusakiewicz, J. J., Rouzer, C. A., and Marnett, L. J. (2002) Isoform-selective interaction of cyclooxygenase-2 with indomethacin amides studied by real-time fluorescence, inhibition kinetics, and site-directed mutagenesis, *Biochemistry 41*, 9654−9662.
21. Gierse, J. K., Koboldt, C. M., Walker, M. C., Seibert, K., and Isakson, P. C. (1999) Kinetic basis for selective inhibition of cyclooxygenases, *Biochem. J. 339* (Part 3), 607−614.
22. Kulmacz, R. J., and Lands, W. E. (1985) Stoichiometry and kinetics of the interaction of prostaglandin H synthase with antiinflammatory agents, *J. Biol. Chem. 260*, 12572−12578.
23. Copeland, R. A. (2000) *Enzymes: A Practical Introduction to Structure, Mechanism, and Data Analysis*, 2nd ed., Wiley-VCH, New York.
24. Kalgutkar, A. S., Marnett, A. B., Crews, B. C., Remmel, R. P., and Marnett, L. J. (2000) Ester and amide derivatives of the nonsteroidal antiinflammatory drug, indomethacin, as selective cyclooxygenase-2 inhibitors, *J. Med. Chem. 43*, 2860−2870.
25. Thuresson, E. D., Lakkides, K. M., Rieke, C. J., Sun, Y., Wingerd, B. A., Micielli, R., Mulichak, A. M., Malkowski, M. G., Garavito, R. M., and Smith, W. L. (2001) Prostaglandin endoperoxide H synthase-1: the functions of cyclooxygenase active site residues in the binding, positioning, and oxygenation of arachidonic acid, *J. Biol. Chem. 276*, 10347−10357.
26. Schneider, C., Boeglin, W. E., Prusakiewicz, J. J., Rowlinson, S. W., Marnett, L. J., Samel, N., and Brash, A. R. (2002) Control of prostaglandin stereochemistry at the 15-carbon by cyclooxygenases-1 and -2. A critical role for serine 530 and valine 349, *J. Biol. Chem. 277*, 478−485.
27. Weggen, S., Eriksen, J. L., Das, P., Sagi, S. A., Wang, R., Pietrzik, C. U., Findlay, K. A., Smith, T. E., Murphy, M. P., Bulter, T., Kang, D. E., Marquez-Sterling, N., Golde, T. E., and Koo, E. H. (2001) A subset of NSAIDs lower amyloidogenic Abeta42 independently of cyclooxygenase activity, *Nature 414*, *212*−*216*.

BI048534Q